DESIGN AND TESTING OF A SUBSCALE SUPERSONIC AEROPROPULSION WIND TUNNEL

The member of the Committee approved the masters thesis of Joji Matsumoto

Frank K. Lu _____

Supervising Professor

Donald R. Wilson _____

Dora E. Musielak _____

DESIGN AND TESTING OF A SUBSCALE SUPERSONIC AEROPROPULSION WIND TUNNEL

by

JOJI MATSUMOTO

Presented to the Faculty of the Graduate School of

The University of Texas at Arlington in Partial Fulfillment

of the Requirements

for the Degree of

MASTER OF SCIENCE IN AEROSPACE ENGINEERING

THE UNIVERSITY OF TEXAS AT ARLINGTON

May 2000

ACKNOWLEDGMENTS

I would like to thank God our father for all the talents and opportunities I have received. I could not finish this thesis without love and support of my parents through all the years since preschool. I thank Gene and Dee Robinson for their care. I would like to show my appreciation to the guidance and patience of advisors, Dr. Frank Lu and Dr. Donald Wilson over three years of the program. I want to thank to Jim Holland for machining and assembly work, Scott Stuessy for welding, Chris Roseberry for practical advice in mechanical designs and electrical problems, Yu Matsutomi for carpentry works and Chul Han Kim for encouragement. This research and development is supported by The State of Texas.

April 10, 2000

ABSTRACT

DESIGN AND TESTING OF A SUBSCALE SUPERSONIC AEROPROPULSION WIND TUNNEL

Publication No. _____

Joji Matsumoto, M.S.

The University of Texas at Arlington, 2000

Supervising Professor: Frank K. Lu

A sub-scale blowdown wind tunnel for aeropropulsion experiments was developed at the Aerodynamics Research Center of The University of Texas at Arlington. The tunnel is capable of Mach 1.5 to 4 and has up to 2 s of run time. The size of the test section is 0.15 x 0.15 m. The tunnel components were newly designed and assembled to be incorporated with an existing supersonic nozzle, a storage tube and a high-pressure compressor. A PC-based preprogrammed controller was also developed to overcome the slow response of a valve controller. An ideal valve opening profile for a particular test is developed based on preceding test results at the same test conditions and storage tank pressure. After several tests and corrective interpolations, the pressure disturbances in the plenum chamber are typically reduced to 1 percent of the stagnation pressure. A preliminary test was conducted at Mach 2.5 and Reynolds number of 63 x 10^6/m, with a stagnation pressure of 928 kPa.

TABLE OF CONTENTS

LIST OF FIGURES

LIST OF TABLES

LIST OF ABBREVIATIONS

A	cross sectional area
E	voltage output signal
M	Mach number
n	polytropic exponent
P	pressure
R_{el}	unit Reynolds number
t	time
t_{run}	run time
Δt	delay of time
T	temperature
U	velocity of air
V	volume
γ	specific heat ratio
χ	factor of pressure drop
ρ	density of air

Subscripts

av	time averaged value
S	storage tube
t	total value
0	stagnation value

1	plenum chamber
2	test section

Superscripts

e	end of test window
i	initial condition of a test
j	j-th run
f	final condition of a test
*	nozzle throat

CHAPTER 1

INTRODUCTION

Supersonic wind tunnels (SWT) have been used for research and development for more than five decades. Aerodynamics, propulsion and acoustic testing are some of the main uses of such tunnels. For example, wind tunnels were used extensively to investigate the aerodynamic characteristics of the Space Shuttle and Concorde. Despite the heavy dependence on computational fluid dynamics (CFD) for modern aerospace vehicle design, wind tunnels have been improved and are still in continuous use. There are many areas where CFD cannot give accurate solutions such as in unsteady flows. Wind tunnel testing can provide crucial data in such difficult flow fields.

Experimental aerodynamics research at the University of Texas at Arlington has been undertaken at the Aerodynamics Research Center (ARC) since 1986. The Center has the following facilities, a low-speed wind tunnel, a transonic Ludwieg wind tunnel, a detonation-driven hypersonic shock tube and an arc-heated tunnel. Many of them were donated from other research facilities and refurbished. The construction of the supersonic wind tunnel was started as part of a continuing improvement program. With completion of the tunnel, ARC has a seamless testing capability from low-speed to hypersonic.

1.1 PRINCIPLES OF SUPERSONIC BLOWDOWN TUNNEL

The supersonic wind tunnel, in general, falls into four categories, blowdown tunnel with a high-pressure gas storage tank, high-enthalpy tunnel with a shock tube, atmospheric-entry wind tunnel with a vacuum pump, and continuous flow wind tunnel with a compressor. The first two types of wind tunnels were possible to develop at the ARC using existing equipment, namely a storage tube, a supersonic nozzle and a high-pressure compressor. A blowdown tunnel was chosen since it has, in general, a longer run time. However, it requires higher construction cost than a shock tunnel to control the pressure in a settling chamber. The idea of creating a supersonic jet using a high-pressure (or low-pressure) gas and a supersonic nozzle is quite old. The Swedish engineer, Carl G. P. de Laval,

discovered the concept of the nozzle in the late nineteenth century. He invented a single stage turbine driven by hot steam through a unique convergent-divergent (CD) nozzle. In Europe, the convergent-divergent nozzle is known as the de Laval nozzle. NACA Langley developed the first blowdown tunnel in 1927. High-pressure air was stored in a large volume tank and a jet through a small pipe was used for testing [1].

A typical blowdown tunnel consists of a storage tank filled with high-pressure air and a CD nozzle. Blowdown tunnels require increasingly higher pressure as the Mach number increases. The starting pressure is experimentally found to be about twice the normal shock pressure loss. A tunnel is started with the opening of an automatic pressure regulator at the end of a storage tank. The high-pressure air in the storage tank expands and settles down in a plenum chamber, where the air slows down and is kept at a constant pressure. Downstream of the plenum chamber is a CD nozzle. It accelerates the flow to supersonic jet. The jet is then decelerated by a diffuser and exhausted to the atmosphere.

1.2 OBJECTIVES

A supersonic blowdown wind tunnel was designed, fabricated and tested. The tunnel will be used to support research such as supersonic inlets and nozzles, and external aerodynamics. Although the existing nozzle has a Mach number range of 1.5 to 4, the design is optimized for operations at Mach 3. The tunnel is designed to have about 5 s of run time with less than 5 percent of turbulence across the test section. After tunnel fabrication, a data acquisition system and operating software were developed.

CHAPTER 2

DESIGN AND CONSTRUCTION OF WIND TUNNEL

2.1 AIR SUPPLY SYSTEM

2.1.1 COMPRESSOR

The high-pressure air supply of the ARC comes from a 1,250 HP electric powered 19.4 MPa (2,800 psi), 5-stage Clark Model CMB-6 compressor (figure 2.1 *(1)*). The air is pumped up to 13.9 MPa (2,000 psi), which is the maximum pressure of the storage tanks (figure 2.1 *(2)*). A low-pressure compressor, rated at 1.3 MPa (175 psi), is used to actuate the valves. Inter-stage coolers and a twin-tower dryer are used to remove moisture from the air. After passing through an after-cooler, the air is stored in three storage tanks, with a total volume of 4.5 m^3 (158.6 ft^3). At full load, the compressor can deliver a flow rate of 1.1 kg/s (1,800 scfm). It takes about 15 minutes to charge all the storage tanks at the maximum pressure. The dry air is then distributed to all of the ARC's facilities.

(1) CMB-6 compressor. *(2) Storage tanks and dryers.*

Figure 2.1. Compressor complex. (1) CMB-6 compressor. (2) Storage tanks and dryers.

2.1.2 STORAGE TUBE

A storage tube was available for the SWT (figure 2.2). The size and maximum pressure of the tube limits the run time of the tunnel. This tube is 292 mm (11.5 in.) in diameter, 26.82 m (88 ft) in length, has a volume of 1.8 m^3 (63.5 ft^3) and is rated for a pressure of 5.27 MPa (750 psi). The three tanks of dry air have sufficient volume to fill the storage tube about 4 times. By charging the main storage tanks twice, it is estimated that the supersonic wind tunnel is capable of achieving a maximum of eight runs daily.

Figure 2.2. Storage tube.

The storage tube is filled from the high-pressure storage by two solenoid valves at an air distribution panel. The solenoid valves are activated manually from a control room, which is protected from the test area by a 178 mm (7 in.) concrete wall. The high-pressure air passes through a 19 mm (0.75 in.) pipe from the back of the panel to the storage tube. The pressure in the tube is closely monitored during a filling process.

2.1.3 ESTIMATE OF RUN TIME

Runtime of a blowdown tunnel with a pressurized tank and a throat is calculated using equation 2.1 [2]. In this equation, the run time is only a function of the conditions in the storage tank and the nozzle throat area.

$$t_{run} = \frac{A^* P_{t1} \sqrt{T_{t1}}}{0.0325 V_2 P_{t1}^2} \left\{ 1 - \left(\frac{P_1}{P_{t1}} \right)^N \right\} \qquad (2.1)$$

This equation gives a good estimate for a tunnel with a long runtime. For a wind tunnel with a short runtime, several additional factors were considered. The starting process requires air to fill the plenum chamber up to a set point pressure. The amount of air that will be wasted in this process is assumed to be about twice of the volume of the plenum chamber. The effective mass of the air in the storage tube is

$$\rho U A t_{run} = \rho_S{}^{i} \cdot V_S - \rho_S{}^{f} \cdot V_S - 2\rho_{t1} \cdot V_1 \tag{2.2}$$

The pressure drops through the automatic valve and the wide-angle diffuser, represented by (1-χ), are assumed to be roughly 40 percent [2]. Thus, equation 2.2 becomes

$$t_{run} = \frac{0.03526\sqrt{T_{t2}{}^{i}}\,P_S{}^{i}}{A^{*}T_2\left(\frac{P_{t2}}{\chi}\right)}\left\{V_S - \left(\frac{\left(\frac{P_S{}^{f}}{\chi}\right)}{P_S{}^{i}}\right)^{1/n}(V_S + 2V_1)\right\} \tag{2.3}$$

The run time of a blowdown tunnel with a small storage volume is shown in figure 2.3. Blowdown tunnels are usually designed to have run time of 20 to 40 s to provide stable measurement of pressures and loads. It is

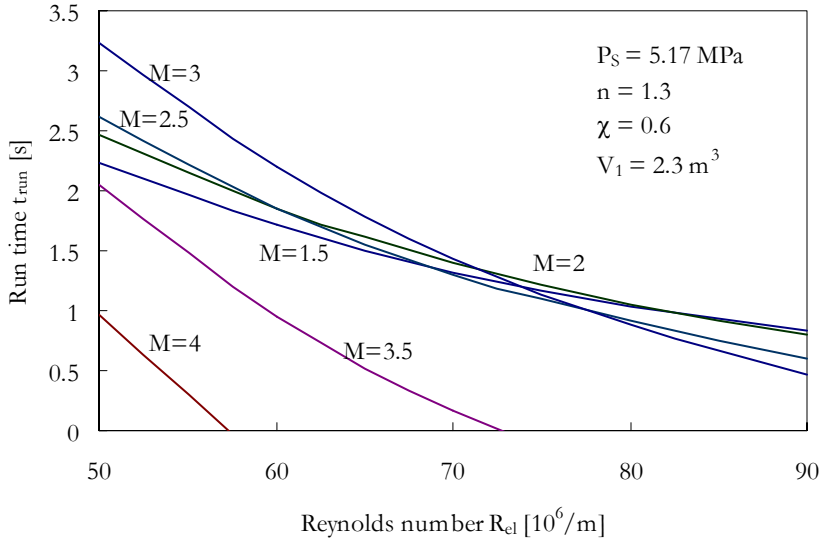

Figure 2.3. Estimate of run time.

important to accommodate cost of construction, runtime and quality of the flow, since the run time decreases as much as 1 s as the length of plenum chamber increases 1 m. The length of the plenum chamber and flow quality are discussed in section 2.2.4.

2.2 TUNNEL COMPONENTS

A schematic of the wind tunnel is shown in figure 2.4. All the tunnel components except storage tube, nozzle and test section were newly designed in-house. The gate valve and the automatic valve were obtained commercially. The tunnel between the storage tube and plenum chamber is rated at 5.27 MPa (750 psig), the nozzle is rated at 3.46 MPa (500 psig) and the rest of the parts are rated at 2.11 MPa (300 psig). The newly acquired parts were designed according to the ASME pressure vessel code [3] and made from SA-516(70) carbon steel that has high allowable stress at low temperature compared to structural steels. The wide-angle diffuser, plenum chamber

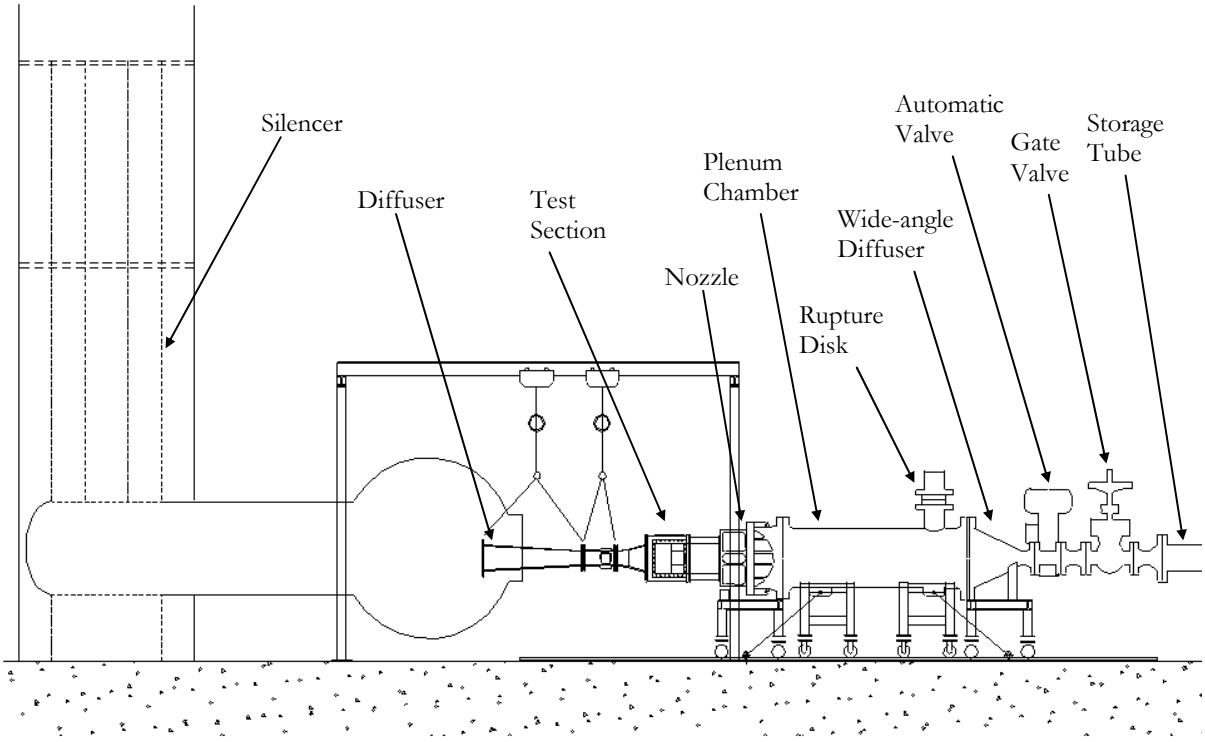

Figure 2.4. Schematic of supersonic wind tunnel.

and nozzle are supported by an individual stand with four grooved casters on two rails to ensure an easy access into the tunnel. The tunnel is anchored to the concrete floor at three points, the bottom end of the storage tube and both bottom ends of the plenum chamber. Six 19 mm (0.75 in.) diameter, 178 mm (7 in.) long wedge bolts anchor down three steel anchor plates. Each plate is connected to the tunnel with a 31.7 mm (1.25 in.) diameter turnbuckle.

2.2.1 GATE VALVE

The storage tube, located at upstream end of the supersonic tunnel, is isolated from the rest of the tunnel by a 152 mm (6 in.) diameter F2064C02TY-600#RF bolted bonnet gate valve (Velan, Canada) (figure 2.5).

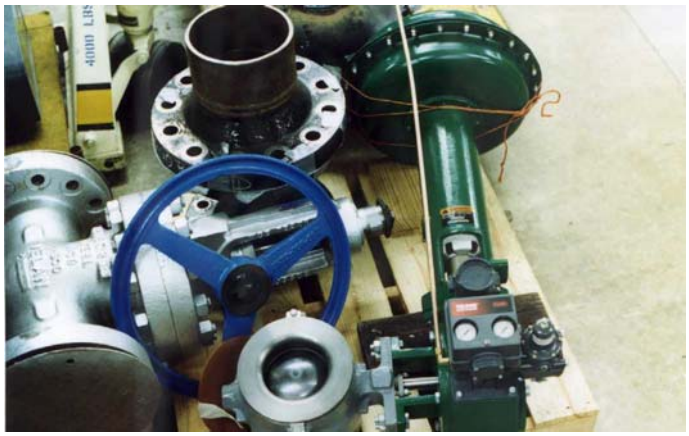

Figure 2.5. Gate valve and automatic valve.

2.2.2 AUTOMATIC VALVE

The flow is started when the 152 mm (6 in.) diameter V200-DVC5020 automatic ball valve (Fisher Controls, Iowa) is opened. Since the storage tank pressure and temperature are continuously dropping during a test, the valve must open continuously to maintain a constant pressure in the plenum chamber. A Rosemount Model 1151GP pressure transmitter is installed at the downstream end of the plenum chamber. It has a pressure range of 0-2.9 MPa (0-400 psig) and an output range of 0-40 mA. A Fisher DPR-950 digital valve controller operated by an air supply at 342 kPa (35 psig) converts an input current signal from the pressure transmitter to a pneumatic output pressure

which rotates the ball valve to the desired degree of opening. The controller can be tuned up using non-linear gains and feedback loops to minimize the starting process and pressure fluctuations during a test. Details of the controller are discussed further in chapter 3.

2.2.3 WIDE-ANGLE DIFFUSER

A wide-angle diffuser decelerates the high-speed flow from the storage tube to a low speed and recovers some portion of the dynamic pressure. Several designs are shown in figure 2.6. Reference 2 shows that models *(1)* and *(2)* work relatively poorly and *(3)* and *(4)* work well. Type *(3)* was chosen as a base model in the present design. A schematic of the wide-angle diffuser is shown in figure 2.7. The included angle of the diffuser is 45 deg. The diffuser encloses a 60 deg angle perforated cone facing into the pipe from the plenum chamber. The cone is made from six triangle plates welded together. The cone contains about one thousand oval holes to spread the jet from

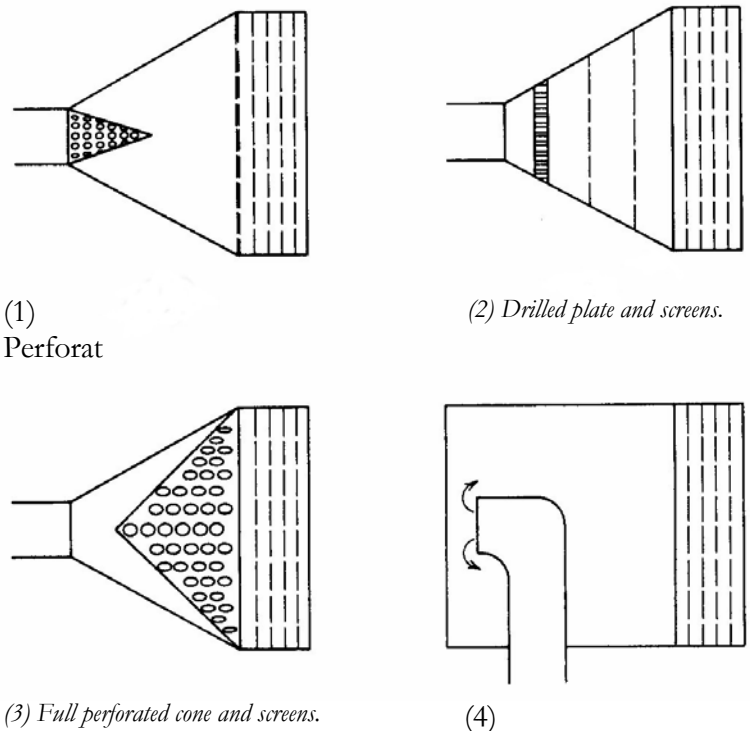

Figure 2.6. Design of wide-angle diffuser. (1) Perforated can plus perforated plate and screens. (2) Drilled plate and screens. (3) Full perforated cone and screens. (4) Reverse entry and screens.

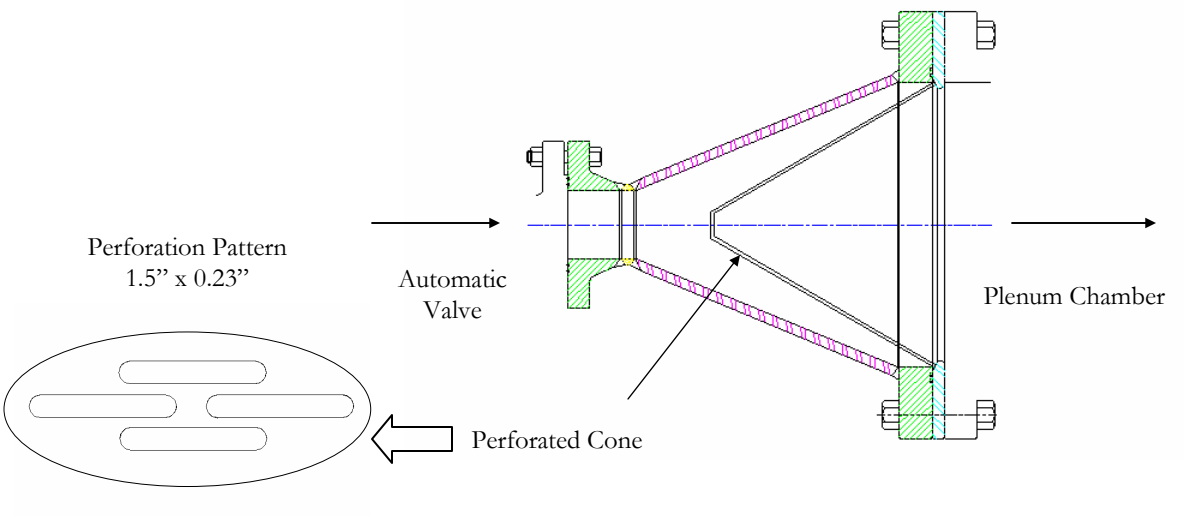

Figure 2.7. Schematic of wide-angle diffuser.

the pipe into a uniform distribution of small jets. The cone reduces the large-scale turbulence and asymmetrical flow leaving the automatic valve.

2.2.4 PLENUM CHAMBER

The quality of the flow into the test section depends heavily on the uniformity of the flow in the plenum chamber. The schematic of the plenum chamber is shown in figure 2.8. The plenum chamber has a pressure rating of 3.55 MPa (500 psi). Uniform flow can be achieved by having a large section area although this is limited by the existing nozzle geometry. With this in mind, the plenum chamber is designed to be 0.609 m (24 in.) in diameter and 2.13 m (7 ft) in length. The flow in the plenum chamber is estimated to have an average speed of 1.5-15.2 m/s (5-50 ft/s). The maximum flow speed is less than the 24.4-30.5 m/s (80-100 ft/s) recommended by Pope and Goin [2]. The lower limit is less than the recommended value of 3.0 m/s (10 ft/s), which causes some heat convection from the wall to the adjacent air. Although this is an important consideration for high-temperature blowdown wind tunnels, it is not felt to be a critical issue for the present design.

In addition to having an adequate length to reduce turbulence, three screens are located in the middle of the plenum chamber. The Mesh Number of the screens is 40, 40 and 50 from upstream to downstream (figure 2.9). Each screen is placed 152 mm (6 in.) from the adjacent screen. These screens are used to damp out turbulence and promote flow uniformity. The effect of damping screens has been reported in reference 4. The results indicate that the turbulence decreases exponentially in a certain distance downstream of a screen and the magnitude of the damping is proportional to the pressure drop between the screen. The screens are installed from the upstream end of the plenum chamber and fixed by the four small steel plates welded in the chamber. Each screen is made from two thin hoops with close fitting. A wire cloth is inserted between the rings and three clamps are used to slide one ring into the other. Then six rivets are inserted around the rings to fix the position of the two rings. Epoxy is applied in the gap, which tautly holds the stretched wire cloth.

Downstream of the screens are four 25.4 mm (1 in.) diameter ports for housing probes to monitor the plenum pressure and temperature and for other purposes such as injection of seed material. The static pressure of the chamber is higher than that of any other downstream portion of the tunnel. In addition, the downstream

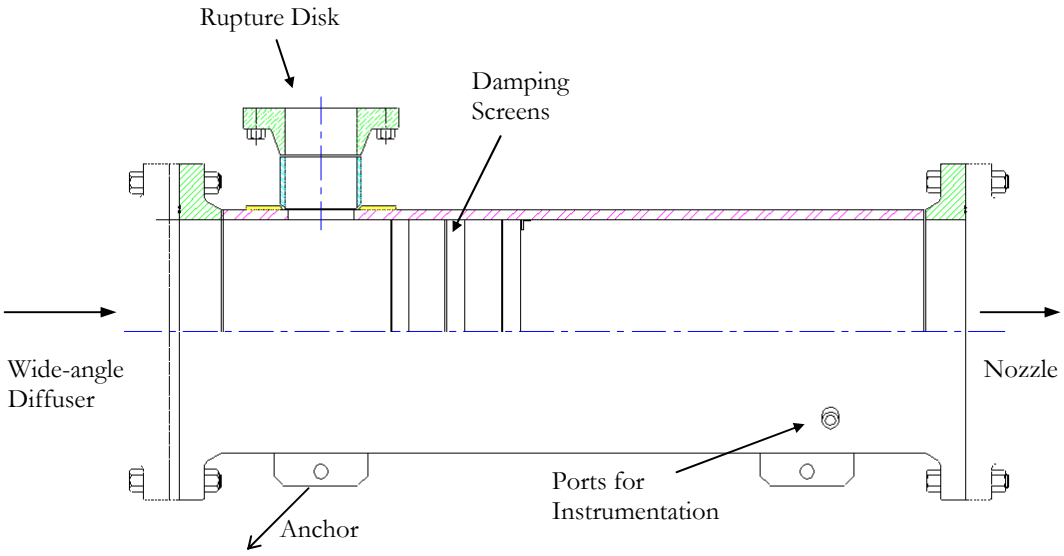

Figure 2.8. Schematic of plenum chamber.

Figure 2.9. Damping screens.

portion of the wind tunnel is designed for a lower rated pressure. Thus in order to protect the facility from catastrophic failure due to over pressurization, a 0.20 m (8 in.) rupture disk, rated at 1.65 MPa (225 psi), is installed near the upstream end of the plenum chamber.

2.2.5 NOZZLE

The variable-area supersonic nozzle (figure 2.10), AMRAD Model GF-6 was obtained as a donation from the LTV Aerospace and Defense Company, Dallas, Texas (presently Lockheed Martin Missile and Fire Control Systems). The nozzle is hand actuated and has a Mach number range of 1.5 to 4.0. The maximum pressure rating of the nozzle is 2.5 MPa (350 psi). It is symmetric in the vertical and horizontal direction. The area converges horizontally at the entrance and vertically at the throat. The overall length of the nozzle is 889 mm (35 in.). The nozzle consists of a rigid contoured throat section and downstream flexible plates. The throat area can be preset to a fixed position prior to a test for fixed Mach number operation. The throat section is designed to move about a pivot, which causes the flexible plates to closely match the nozzle contour determined by the method of characteristics. This provides a uniform exit flow over the entire Mach number range of the nozzle. The nozzle exit has a 152 mm (6 in.) square cross section.

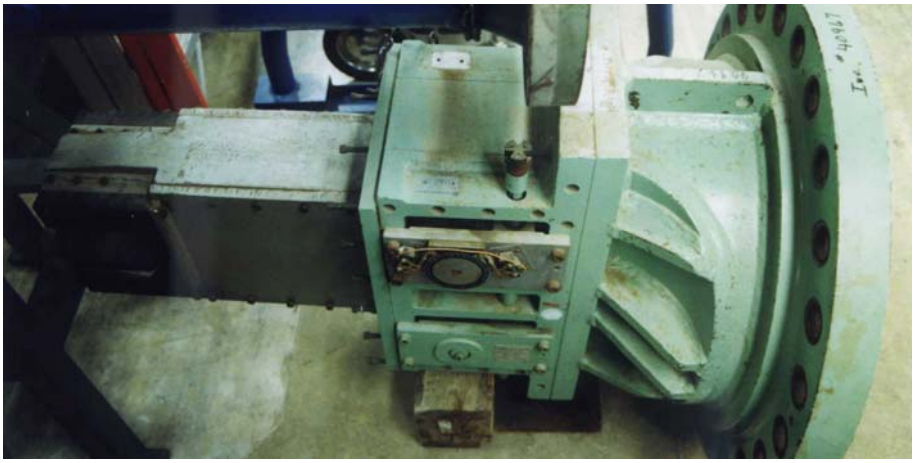

Figure 2.10. AMRAD supersonic nozzle.

2.2.6 TEST SECTION

The primary consideration in constructing the test section is to make sure that the test section can enclose a relatively large sub-scale engine model. Therefore, an enclosed free jet was chosen for the test section, unlike a conventional solid wall design. A side view of the test section is shown in figure 2.11. This test section was originally used by LTV for semi free jet inlet model tests with an angle of attack. It was modified presently for fixed angle of attack testing.

The advantage of a free jet test section is that the larger cross sectional area at the test section minimizes choking and this makes it possible to install relatively large test models. According to reference 5, a test section with a longer free jet length requires a higher starting pressure. Adding or subtracting an adapter piece between the nozzle and the test section can modify the free jet length. The test section is enclosed by a 280 mm (11 in.) by 445 mm (17.5 in.) casing, with 324 mm (12.7 in.) by 343 mm (13.5 in.) glass windows on the two sides of the test section to provide substantial optical access. The free jet has a 152 mm (6 in.) square section and it is 343 mm (13.5 in.) long. A model can be attached to a strut and installed from the top opening of the test section. It is also possible to mount models through attachments in the diffuser.

Figure 2.11. Test section.

2.2.7 DIFFUSER

The diffuser captures the flow from the test section. One of the factors that contribute to an increase in the power requirement of a supersonic wind tunnel is the aerodynamic irreversibility in the diffuser. A typical constant area diffuser consists of a conventional subsonic geometry diffuser preceded by a long constant area duct. This type of diffuser gives nearly the same recompression ratio as a normal shock even though the geometry is quite simple compared with a variable area diffuser. The compression occurs through a system of oblique shocks interacting with the boundary layers. This is not the most efficient way to recover the pressure but it is often more practical and very stable under different Mach numbers. It is possible to design more efficient ducts for specific conditions, but they may perform poorly at off-design points. Based on results from reference 6, the diffuser geometry chosen for the present wind tunnel includes a 335 mm (14 in.) convergent entry section, 380 mm (15 in.) of constant area duct followed by a 0.97 m (38 in.), 6 deg. angle divergent diffuser (figure 2.12). The diffuser throat cross section is a 152 mm (6 in.) square. The throat area is much larger than that of the nozzle, so that a calibrated ASME mass flow pipe can be inserted through the diffuser throat for determining the pressure recovery versus mass flow characteristics of

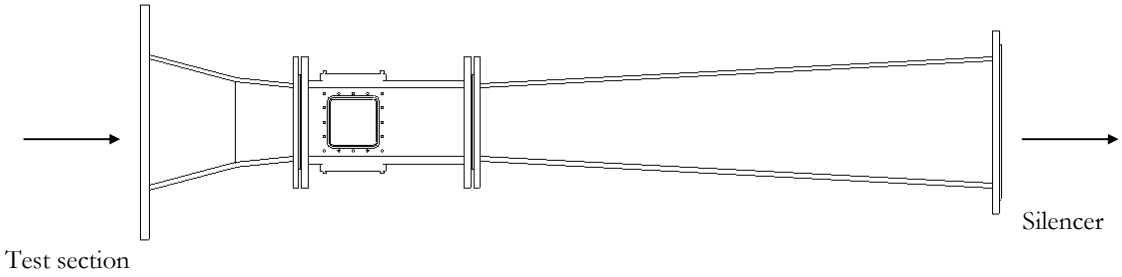

Figure 2.12. Schematic of diffuser.

supersonic inlets. In addition, the diffuser efficiency is not strongly affected by the throat area, although, for a larger throat, a longer constant duct throat is necessary to reduce the flow to subsonic speed.

2.2.8 SCAVENGER SCOOP

The scavenger scoop is the duct in the diffuser, which is used to support probes or to vacuum the air out of an engine model in the starting process. The outer diameter of the scoop is 63.5 mm (2.5 in.) and the length is 1.14 m (45 in.), as shown schematically in figure 2.13. The scoop is made of six aluminum tapered sections and one straight steel pipe. Two steel wings are extended from the scoop to an outer casing to support the scoop at the centerline of the tunnel. The scavenger scoop is usually used for ramjet and turbojet engine testing. It collects the

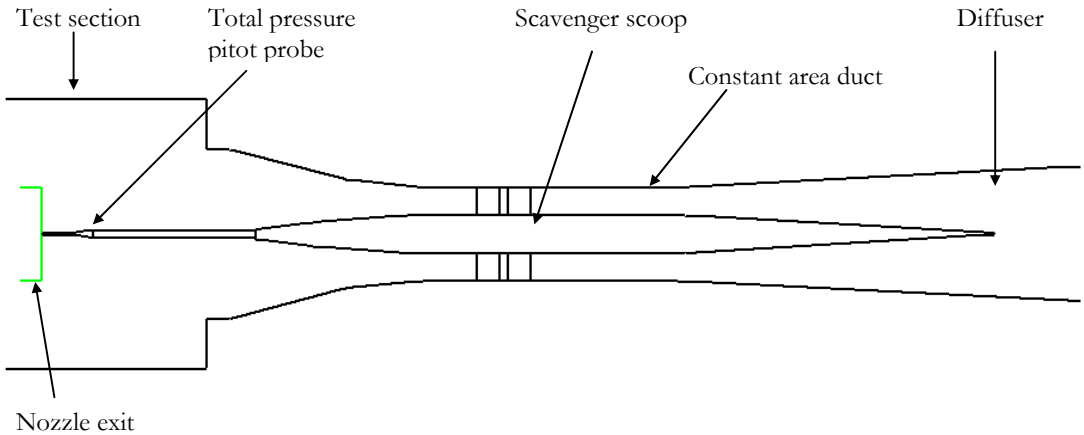

Figure 2.13. Schematic of scavenger scoop.

engine exhaust gases. Although the primary purpose of this tunnel is not engine testing, the large area duct with a scoop has several advantages over a narrow duct with the same opening area. The biggest advantage is that it reduces the length of the shock duct. The required shock duct length to reduce supersonic flow down to subsonic is a function of the Mach Number and the width of opening of the duct [7]. It is possible to have a small width of duct with the same opening area. The narrower gap means the boundary layers contract the flow faster. Another advantage is that it can be used to mount pressure probes or models over the extended arm from it. A vacuum line can be also included in the duct for nozzle tests to take a bow shock sitting at a model into the diffuser during a starting process. However, it increases the power requirement about 7 % at Mach 3.

2.3 INSTRUMENTATION

The major requirement in implementing a data acquisition system is to obtain adequate data to analyze an experiment in terms of Reynolds number and Mach number. Instead of having unique and very complicated

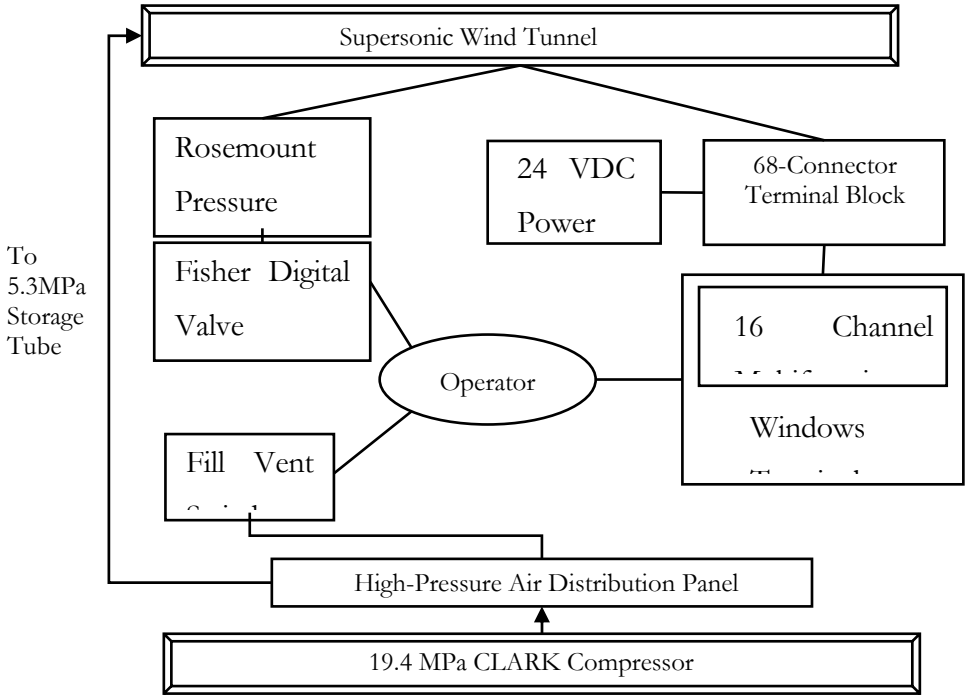

Figure 2.14. Block diagram of tunnel operating system.

systems as it can be seen in many old wind tunnels, a simple and powerful system utilizing commercial off-the shelf components can be implemented. Reference 8 shows the advantage of the modular architecture and graphical interface of the Data Acquisition System (DAQ). Transducers, an A/D converter, and system software are the major components of a DAQ. A PC-based DAQ is installed in a control room that is about 25 m (80 ft) away from the wind tunnel. The pressure transmitter for the automatic valve is also installed in the same room. The signals from transducers are carried through 15-conductor and 25-conductor shielded cables as listed in appendix B. An operator is required to handle three devices (figure 2.14) to start the tunnel. A fill vent switch, which charges and discharges the high-pressure air to the storage tube. Visual interface buttons on a monitor to start and stop acquiring data. Finally, a switch on the transmitter must be pressed to start the opening of the automatic valve.

2.3.1 DATA ACQUISITION SYSTEM

DAQs that are mostly available today are easy to upgrade and also come with many functions and user friendly interfaces. XI and PXI chassis are very popular since they provide high data transfer rate and expandability. A PC-bus based data acquisition system is one of the solutions with much less expense. The PC-based system also eliminates switches and digital panel displays. A multifunction I/O board, PCI-MIO-16E-4 (National Instruments, Austin, TX), is used to collect the data from the transducers. It has 12-bit accuracy, 16 differential analog input channels and a sampling rate of 200 kS/s. Five channels of voltage data from transducers are gathered at a rate of 1 kS/s and are converted to engineering units at real time. Pressure and the Mach number are monitored through the form of graphical interface such as gages and graphs throughout the experiments.

2.3.2 TRANSDUCERS

Four pressure transducers are used for initial testing. All of them are voltage output strain gage transducers which accept 24 VDC excitation and have output ranges of 1-5 or 1-11 V. The transducers are powered by a Hewlett-Packard 6235A triple power supply. Transducer PX613-1KG5V (Omega Engineering, Stanford, CT) is located in the storage tube and is used to monitor the pressure during the filling process. Transducer PX613-300G5V is at the downstream end of the plenum chamber and monitors the stagnation pressure of the flow. These

two transducers are mounted flush to the inside surface of the storage tube and the plenum chamber respectively. Transducer PX613-100G5V is connected to the tip of a pitot pressure probe at the centerline of the test section. Absolute pressure transducer PX-303-050A is used to measure a static pressure at the exit of the supersonic nozzle (mentioned in chapter 4). The response time of all the pressure transducers is 1 ms.

A standard deadweight tester (No. 35260-4 Cenco Instruments Company) is used to calibrate the pressure transducers. The weights and pistons are calibrated to yield 0.1 percent of the indicated pressure. The calibrated pressure is obtained by equation 2.4. Zero balance and linearity of the pressure transducers are shown in table 2.1.

$$Calibrated\ \mathrm{Pr}essure = (Linearity)\cdot\left(\frac{\mathrm{Pr}essureRange}{OutputRange}\right)\cdot(Output) + ZeroOffset \tag{2.4}$$

Table 2.1. Pressure transducers calibration result

Model	Usage	Pressure Range	Output Range	Linearity	Zero Offset	Accuracy	± Error (95%) after calibration
PX-303 050A	P_2	0-334.6 kPa (0-50 psia)	1-11 V	1.0069	-0.9911 kPa (-0.1438 psi)	0.40 % > 0.25 % FS[1]	0.6493 kPa (0.0942 psi)
PX-613 100G	P_{t2}	0-790.6 kPa (0-100 psig)	1-5 V	1.0015	-2.209 kPa (-0.3206 psi)	0.13 % < 0.4 % FS	0.7120 kPa (0.1033 psi)
PX-613 300G	P_1	0-2.169 MPa (0-300 psig)	1-5 V	1.0014	-8.088 kPa (-1.1735 psi)	0.23 % < 0.4 % FS	1.764 kPa (0.2559 psi)
PX-613 1KG	P_S	0-6.994 MPa (0-1000 psig)	1-5 V	1.0008	-26.95 kPa (-3.9094 psi)	0.31 % < 0.4 % FS	42.81 kPa (6.211 psi)

1) Manufacturer specified accuracy

One type T thermocouple, TMQSS-125G-6 (Omega Engineering), is installed at the downstream end of the plenum chamber. The thermocouple wires are protected by a 3.2 mm (0.125 in.) diameter sheath. The thermocouple has a 25 ms response time. The tip of the sheath is immersed about 10 mm (0.38 in.) in the flow Rather than connecting the thermocouple directly to the amplifier circuit, which would create an uncompensated voltage at the dissimilar metal connections, the constantan wire of the thermocouple measuring air temperature is connected to constantan side of a second type T thermocouple. This second thermocouple is placed in a reference ice water bath. This configuration provides copper connections to the amplifier circuit, which do not require any compensation. The output micro-voltage signal is amplified by an op amp up to the maximum input voltage of the data acquisition board (figure 2.15).

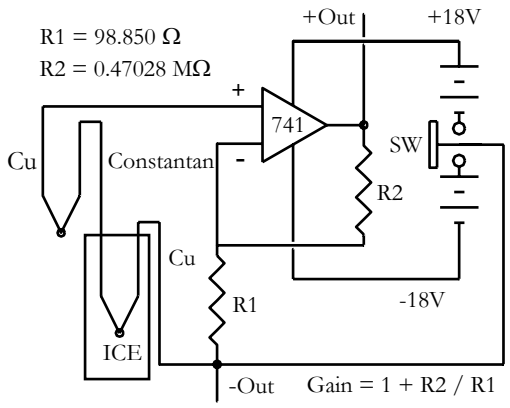

Figure 2.15. Circuit diagram of thermocouple and amplifier.

2.3.3 TOTAL PRESSURE PITOT PROBE

The Mach number of the test section can be determined in three ways. Any two combinations of the static pressure in the test section and the stagnation pressure in the plenum chamber or the stagnation pressure of the pitot probe yields the Mach number. Usually, the first two pressures are used for near sonic operation (equation 2.5).

$$\frac{P_{t2}}{P_1} = \left[\frac{\gamma+1}{2\gamma M^2-(\gamma-1)}\right]^{1/(\gamma-1)}\left[\frac{(\gamma+1)M^2}{(\gamma-1)M^2+2}\right]^{\gamma/(\gamma-1)} \tag{2.5}$$

It is recommended to use the last two pressures above M=1.6 since the total pressure loss becomes sufficient [2]. The Mach number of the test section is then calculated using equation 2.6.

$$M = \left\{\frac{2}{\gamma-1}\left[\left(\frac{P_2}{P_1}\right)^{1-\gamma/\gamma} - 1\right]\right\}^{0.5} \tag{2.6}$$

The pitot probe is a simple tube facing into the flow (figure 2.13). The probe is made of a 3.18 mm (0.125 in.) O.D. brass tube and telescoped tubes that reinforce the tip of the probe. The tip of the probe has an inside-to-outside diameter ratio of 0.464 and it has square edge so that a sharp bow shock is formed at the tip. The probe is enclosed by a 12.7 mm (0.5 in.) stainless steel pipe and that is supported in the scavenger scoop. Sliding the collar on the pipe changes the position of the probe from inside of the nozzle to the nose cone of the scoop.

2.3.4 STATIC PRESSURE PORT

An extension plate with a static pressure port is attached at the exit plane of the nozzle (figure 2.16). The plate is 25 mm (1 in) thick and a 1.6 mm (0.06 in) hole is drilled in the middle of the plate tangent to the nozzle surface. A 3.2 mm (0.125 in) I.D. flexible hose is attached to the hole and led out of the test section so that the top plate is free to move upward as a pressure relief plate (detail in section 4.2). The absolute pressure transducer PX-303-050A is used to measure the static pressure.

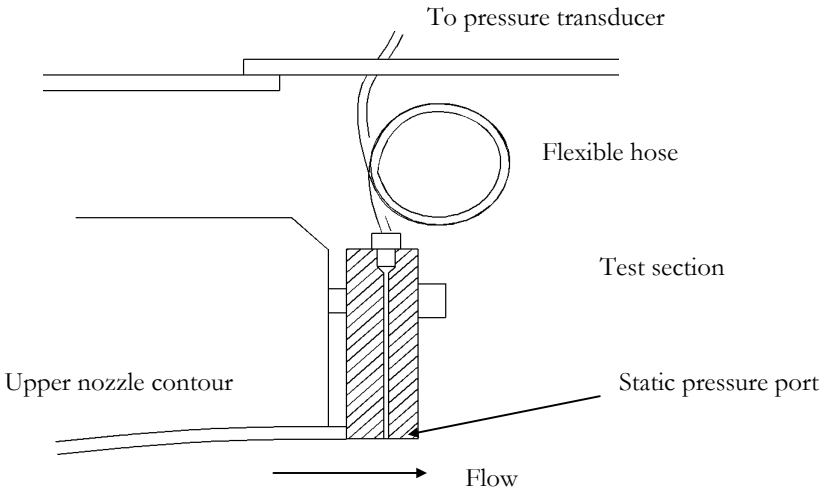

Figure 2.16. Static pressure port.

CHAPTER 3

CONTROLLER

Without exception, blowdown tunnels are intended to be operated at a constant stagnation pressure in the settling chamber. The stagnation pressure is usually controlled by one or more pressure regulators. The regulator valve is opened progressively wider during a run as the storage tank pressure decreases continuously. When SWTs were first developed, they were manually operated. Since that time, many SWTs have been modified to provide better data. Advances in microcomputer and measurement technology have enabled operators to obtain pressures and temperatures that are more accurate and control the SWT using a simple operating system. The type of controller varies among tunnels depending on their size and budget. They vary from a purely mechanical controller using a set of needle valves of different diameters to a pneumatic valve with PID (proportional gain, integral time, and derivative time) control. One of the most advanced wind tunnel operating system uses a real time neural net controller with a parallel processing workstation [9]. This SWT can be operated with as few as three people and has a Mach number deviation of 0.005 and total pressure deviation of 0.7 kPa (0.1 psi) [10].

The primary reason for installing a quality controller to a wind tunnel is that it can significantly improve flow quality in a test section. Good flow quality is essential to provide crucial data to verify CFD analysis, for example. The required accuracy of flow may vary with the type of tunnel. For a typical airplane test, criteria such as less than 1.0 percent of error in Cd and Cp are usually sufficient. To meet those criteria, the Mach number in the test section must stay uniform to about ± 0.3 percent at M = 3.0 [11]. Unlike Mach number, Reynolds number is hard to maintain at a constant value since the temperature of a storage tank drops during a test.

3.1 PID CONTROLLER

Initially, a Rosemount model 1151 pressure transmitter, a Fisher DVC-5000 digital valve controller and a Fisher V200 automatic ball valve were used to control the SWT (figure 3.1). The stagnation pressure in the plenum

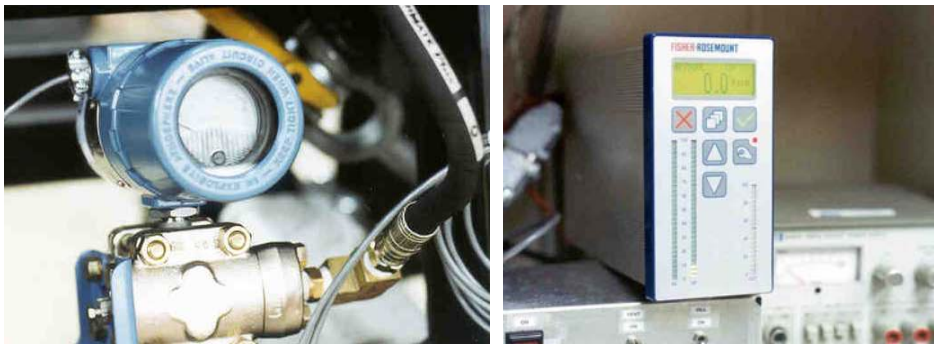

Figure 3.1. Pressure transmitter and digital valve controller.

chamber was converted to a 0-40 mA current signal by the transmitter located 0.6 m (2 ft) upstream from the nozzle. The data was then fed to the digital valve controller. The controller has three parameters that can be changed to maintain a steady plenum pressure, a proportional gain (K_P), an integral time (T_I) and a derivative time (T_D). The digital valve controller compares the stagnation pressure with a set pressure. Then a corrective output signal is derived

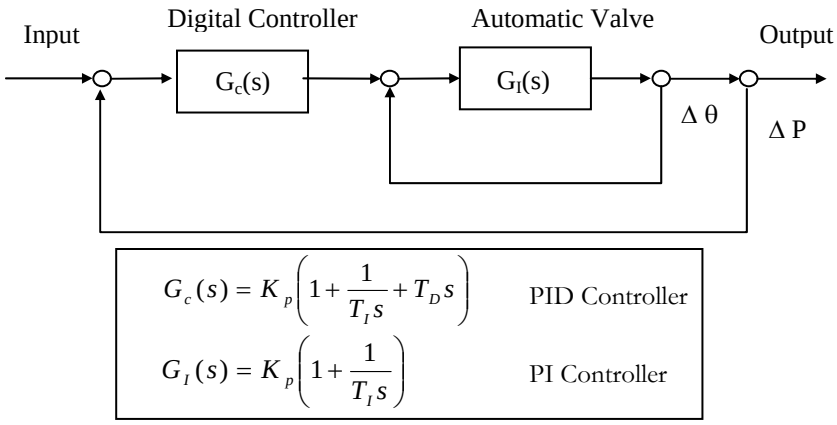

Figure 3.2. PID controller block diagram.

according to the setting of the three parameters. These parameters may be modified to increase the process gain, to minimize an offset between the set point pressure and the pressure reading (ΔP), and to boost the initial starting process respectively. The automatic valve also has a PI controller loop in the circuit so that the error of an actual position of the valve (Δθ) is corrected to match a signal from the valve controller (figure 3.2).

The objectives in setting up the controller parameters for the valve were to minimize the duration of the starting process and to minimize the pressure oscillations around a set point pressure to obtain as long steady run time as possible. Unfortunately, these two goals were not satisfied with a feedback loop controller. Faster system response makes the system more difficult to damp. At first, two parameters, K_P, T_I, for the automatic valve were chosen by trial and error, so that the valve not only moves as fast as possible but also does not cause an overshoot excessively. The second step of the trial-and-error process was to arbitrarily set the three control parameters, K_P, T_I, T_D, and run the tunnel with a low storage pressure and evaluate the results. Changes were then made to one parameter at a time and the setting was tested again to reveal if an improvement occurred. At this stage, a typical oscillation of the stagnation pressure, observed during the refinement process, was 30 to 100 percent of the set pressure, which continued during a run with little decay (figure 3.3). The reasons for the poor performance were considered to be that slow response of

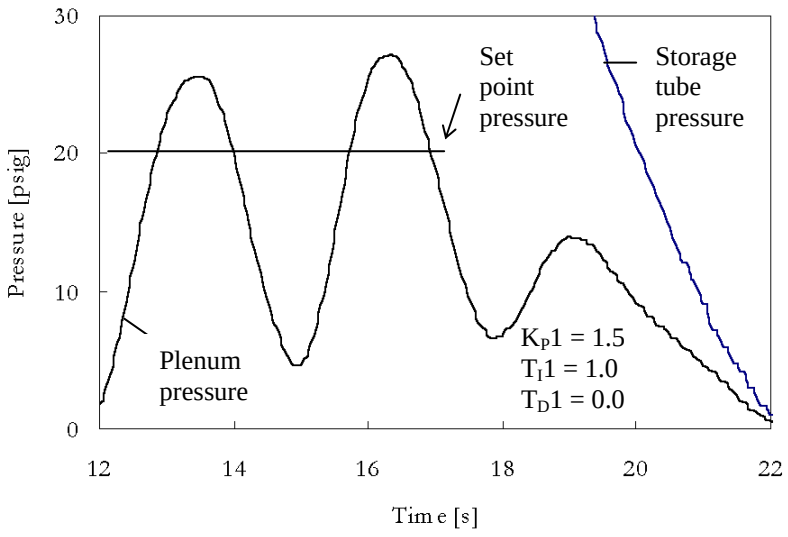

Figure 3.3. Typical plenum pressure trace using PID controller.

the automatic valve, the time-delayed pressure data fed into the control loop, and the processing time delay in the digital valve controller. For these reasons, the system exhibited oscillatory behavior.

Only the response time of the automatic valve could be improved without a major modification. Increasing the flow rate of the supplied actuation air by putting two 1:1 dome pressure regulators shortened the opening and

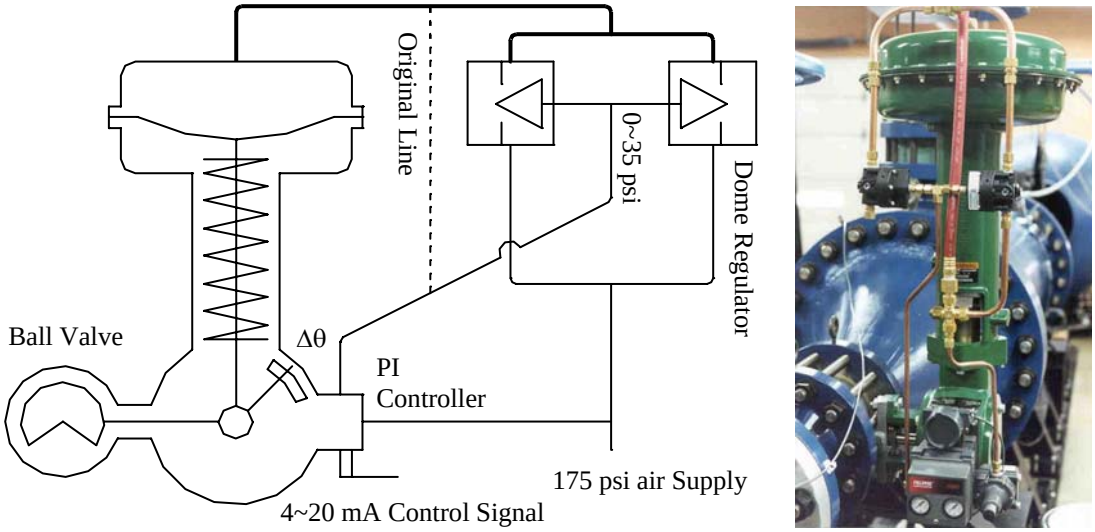

Figure 3.4. Modified pneumatic line of automatic valve.

closing time of the valve from about 10 to 2 sec (figure 3.4). However, a very small improvement in damping the pressure oscillation was recorded after the change. The cause of the oscillation was the time delay of the stagnation pressure data and the slow response of the automatic valve. Some of the time delay was due to the position of the pressure transmitter, which was about 2.4 m (8 ft) downstream from the automatic valve. This caused a 0.25 to 0.6 s delay depending on the test conditions. Instead of putting another pressure transducer, just downstream of the automatic valve, where a high pressure and high-speed jet rumbles by, a radical change in the control system was made.

3.2 PREPROGRAMMED CONTROLLER

Unlike a PID controller, a preprogrammed controller is not strictly a realtime system. The opening profile of the automatic valve is scheduled before a test. During a test, the valve opens according to a predetermined schedule. The advantages of having a preprogrammed controller is that (1) it compensates for the time delay of inputs and slow response devices (2) it shortens the starting process (3) it unifies control and monitoring system and gives more flexibility to the operations. The disadvantage of this approach is that it takes several training test runs to optimize the performance. If experiments are done using consistent storage tank pressure and nozzle settings for all training runs, it is possible to find an ideal valve opening profile for a certain test condition. Fortunately, this change of operation required minimal modifications. The multifunction I/O board PCI-MIO-16E-4 (National Instruments) was used to produce an analog voltage output. The digital valve controller was altered to enable it to convert a voltage signal from the I/O board to a current signal that controls the automatic valve. Once the storage tube was filled with compressed air, the pre-programmed output signals were loaded into the RAM of a computer. As an operator starts the tunnel, the 12-bit control signals were transmitted to the automatic valve at a rate of 500 data/s until the operator stops the test.

3.2.1 CONTROLLER TRAINING PROCESS

The first step of the training algorithm is to guess an initial voltage output profile. The profile has two separate regions; a starting ($0' t \leq 2$ sec) and a steady process ($t > 2$ sec) (figure 3.5). During the starting process, the stagnation pressure in the plenum chamber reaches a set pressure. To better insure starting of the nozzle, the set point pressure was chosen to be at about 10 percent larger than the minimum required starting pressure of a test. The valve was opened rapidly at first. As the stagnation pressure approaches the set point pressure, the valve movement was slowed so that the acceleration of the valve was almost constant in the transition from the starting to the steady process. In the steady process, the valve was opened exponentially to compensate for the large pressure drop in the storage tank.

The second step of the algorithm was to conduct two experiments with the initial setting. The final opening percentage of the valve in the starting process was manually refined with the second experiment. The

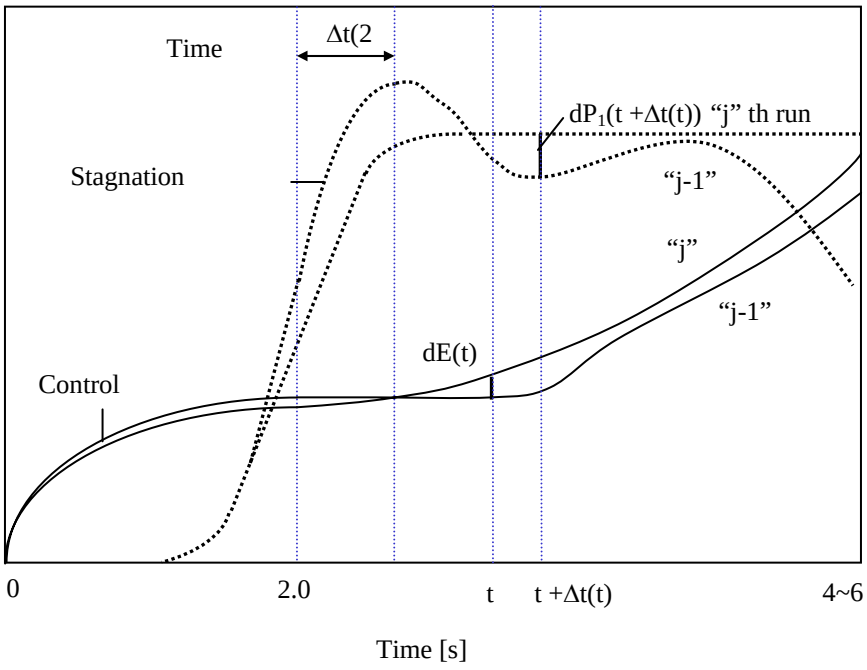

Figure 3.5. Schematic of training procedure of preprogrammed controller.

output signal to the valve and the resulting stagnation pressures were compared between the two experimental trials. With the last two trials, the time delay of the pressure data ($\Delta t(t)$) and the rate of change of the output voltage with respect to the stagnation pressure (dE/dP_1) were determined. The time delay was not constant during the steady process. It was approximated by linear interpolation of the time delay at the end of the starting process ($\Delta t(2.0)$) and the end of the steady process ($\Delta t(t^e)$) as

$$\Delta t(t) = \Delta t(2.0) + \frac{\Delta t(2.0) - \Delta t(t^e)}{2.0 - t^e} \tag{3.1}$$

Since dE/dP_1 is almost constant in the steady process, it was found by comparing the plenum pressure and the output voltage of j-1 th and j th run (figure 3.6),

$$dP_1^j = P_1^j(t) - P_1^{j-1}(t) \tag{3.2}$$

$$dE^j(t) = E^j(t) - E^{j-1}(t) \tag{3.3}$$

$$\frac{dE}{dP_1} = slope\left\{(dE^j(t) - dE^{j-1}(t)), (dP_1^j(t + \Delta t(2.0)) - dP_1^{j-1}(t + \Delta t(2.0))\right\} \tag{3.4}$$

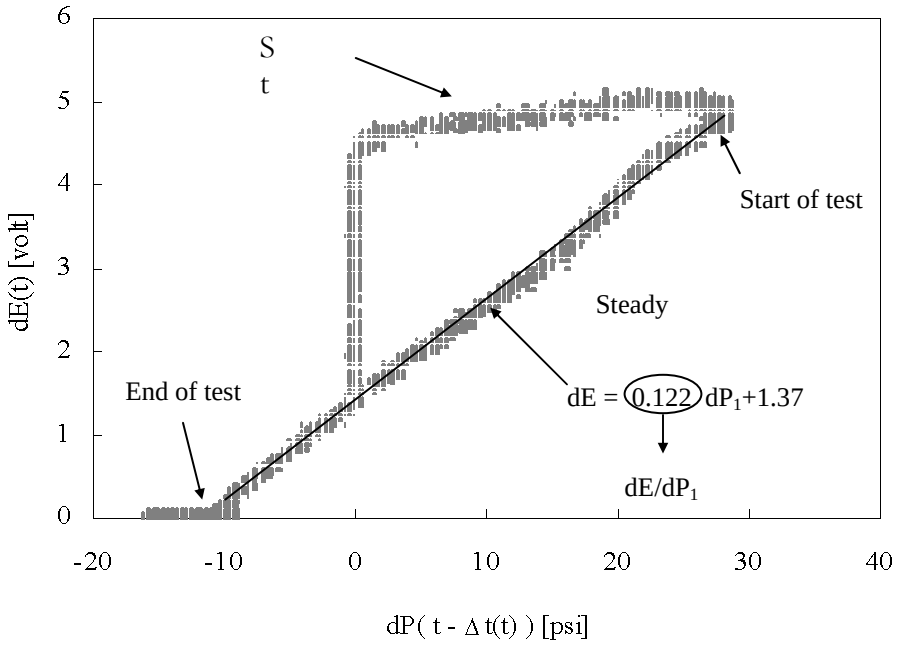

Figure 3.6. Averaged dE/dP_1 for M=2.5.

The pressure data ($dP_1(t)$) was found using a 21-points moving average to reduce noise in the output signal. This last step was continued until the stagnation pressure in the steady process was within a certain accuracy of the set point.

The new output voltage was found by magnifying the original function for the starting process. The original function is the curve which goes through two points of (t, E(t)) = (0, 0) and (2.0, E(2.0)), and also has positive acceleration in $0 < t < 1.0$, and negative acceleration in $1.0 < t \le 2.0$. One of such curves can be expressed as

$$E^j(t) = \frac{E^j(2.0)}{1-\frac{1}{1+2.0}} \cdot \left(1-\frac{1}{1+t}\right) \tag{3.5}$$

Now, the new output voltage is

$$E^{j+1}(t) = \left(\frac{E^j(2.0) - \frac{dE}{dP_1} \cdot dP_1^j(2.0)}{1-\frac{1}{1+2.0}} \right) \left(1-\frac{1}{1+t}\right), (0 < t \le 2.0) \tag{3.6}$$

For the steady process, adjustment of the voltage signal (dE) was added to the old output signal,

$$E^{j+1}(t) = E^{j}(t) - \frac{dE}{dP_1} \cdot dP_1^{j}(t + \Delta t(t)), (2.0 < t) \tag{3.7}$$

The new voltage output profile was saved as a text file and loaded into the computer for the wind tunnel operation. The profile was tested prior to a run without filling up the storage tube. The flow chart of the program is shown in appendix C.

CHAPTER 4

RESULTS

4.1 SHAKEDOWN TESTS

After the modification of the controller, the main focus was to safely start the tunnel and estimate the starting pressure. The storage tube pressure was increased from 2.17 MPa (300 psig) to 4.93 MPa (700 psig). The stagnation pressure in the plenum chamber was kept under 1.14 MPa (150 psig). The control signal was not optimized but manually increased to avoid over pressure in the plenum chamber. The nozzle was set for Mach 2.5. The nozzle was observed to start when the stagnation pressure reached 791 kPa (100 psig) (figure 4.1). The total pressure in the test section jumped up and stayed about 52 percent of the stagnation pressure. The calculated Mach number was about 2.4. However a weak normal shock was thought to be located in the nozzle. To check this hypothesis, the stagnation pressure was increased to push the normal shock out of the nozzle. During a test, the top plate of the test section was

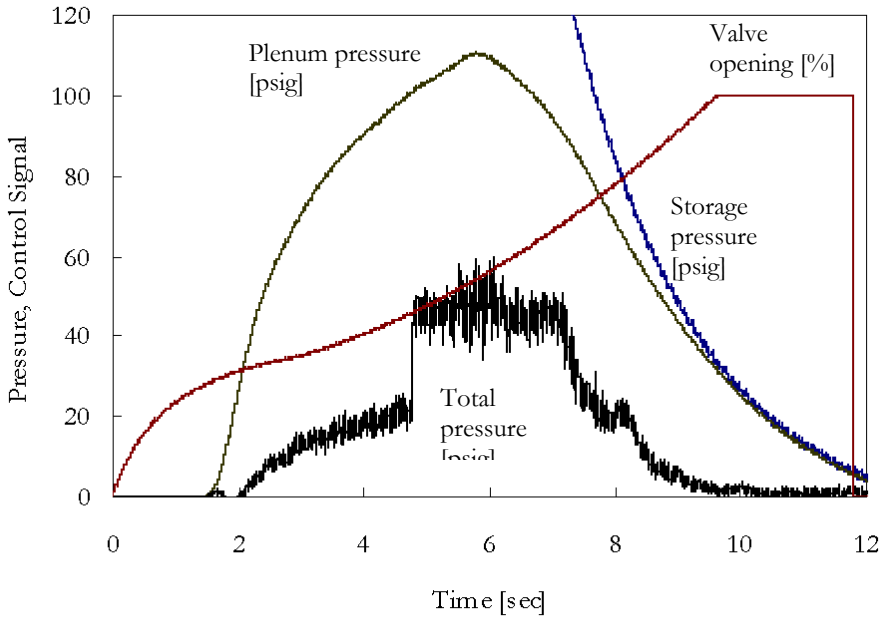

Figure 4.1. Pressure trace of a shakedown test.

blown off because of failure of the bolts holding the hinges. The size of the bolts was increased after the incident and a pressure transducer was attached at the top plate.

4.2 PRESSURE RELIEF PLATE

The total pressure showed the same trend even at the higher stagnation pressure. The reason why the normal shock could not be pushed out of the nozzle was that the static pressure in the test section also increased as the stagnation pressure increased. As a result, the pressure ratio was about the same despite the change. To release the excess pressure in the test section, the top plate of the test section was modified (figure 4.2). Four shafts were pressed into the plate and they were held in position by four linear motion bearings and four supporting towers bolted on the top of the test section. Springs were also inserted to the support so that the plate moves up and down depending on the pressure. After this modification, several tests were conducted to check the spring rate and the movement of the

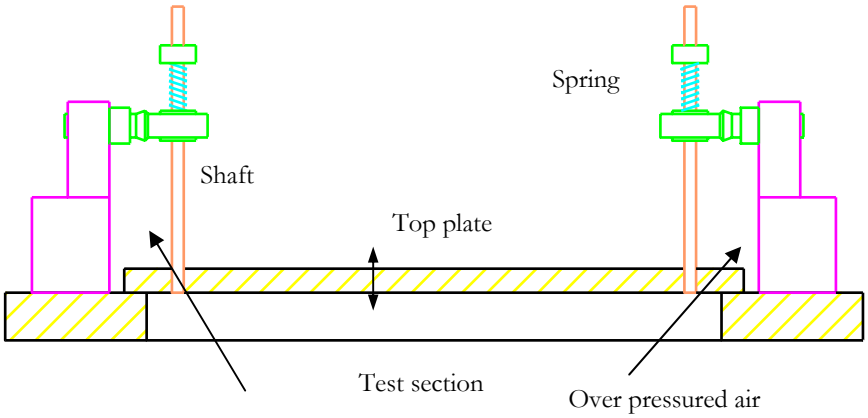

Figure 4.2. Pressure relief plate.

plate. As the pressure in the test section increases, the plate quickly jumped up and down once and was then raised up to the maximum height of 51 mm (2 in.) until the end of the test. Although the plate did not come down during the tests, the nozzle was started (figure 4.3). The pressure in the test section was above ambient at about 255 kPa (37 psia) while the static pressure at the exit plane of the nozzle was reduced to 55 kPa (8 psia). The scavenger scoop was

removed to allow no contraction after the test section. At the next test run, the pressure in the test section was reduced somewhat but it was still above the ambient pressure. This pressurized test section makes an over-expanded free jet exiting the nozzle. In this condition, the Mach number of the test region decreases by strong oblique shocks from the nozzle edges. As a result, the area of test region of uniform Mach number is smaller than the case of an ideal expansion.

4.3 OPTIMIZATION OF CONTROLLER

An optimization of the voltage profile of the control signal was performed for a storage tube pressure of

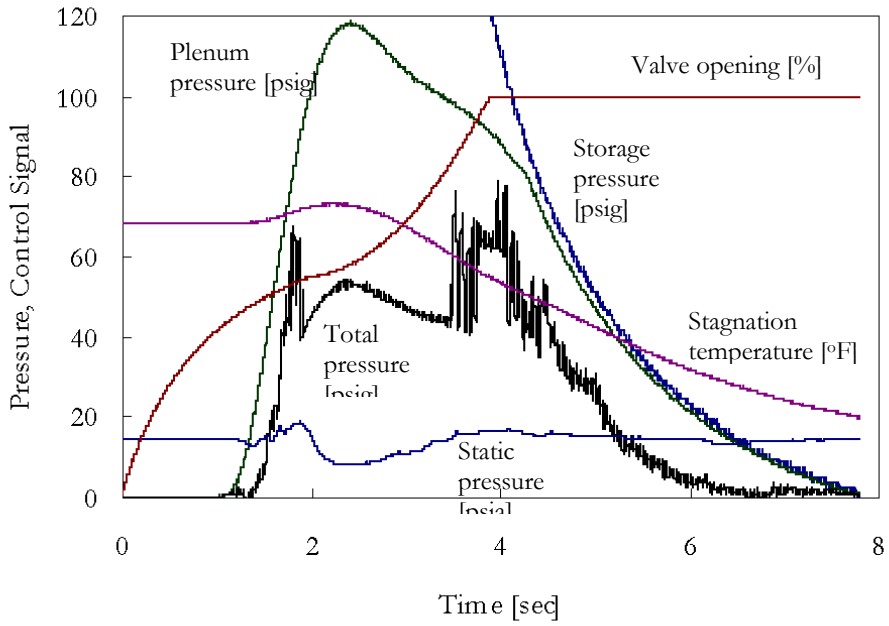

Figure 4.3. Pressure trace of a test with scavenger scoop.

4.93 MPa (700 psig) and the nozzle throat area for Mach 2.5. The stagnation pressure in the plenum chamber was 928 kPa (120 psig). In the first two experiments, the automatic valve was opened 40 percent and 45 percent in 2 s. After 4 more runs of training (figure 4.4), the stagnation pressure was held virtually steady (figure 4.5).

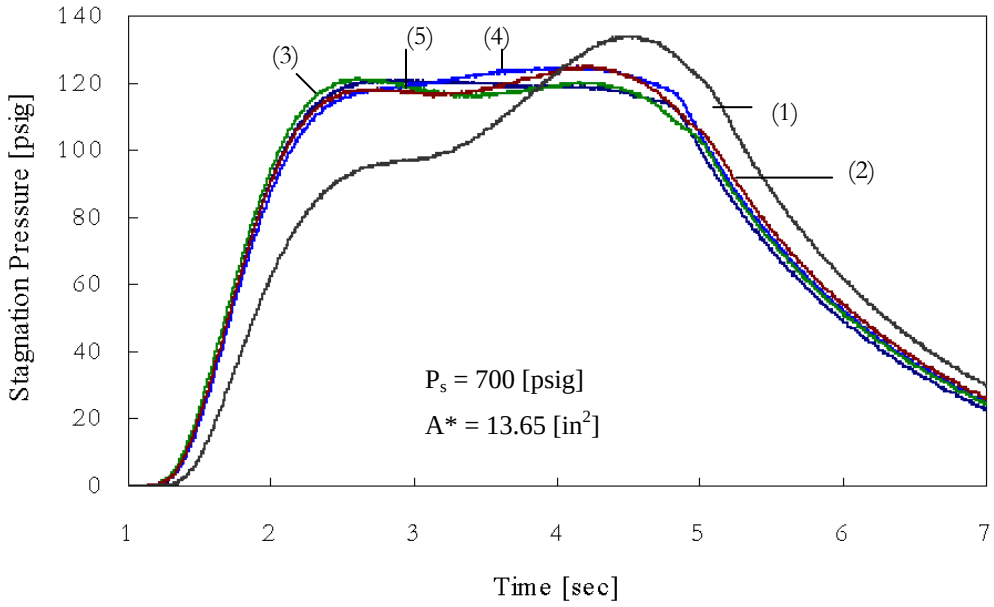

Figure 4.4. Plenum pressure trace of five training processes.

4.4 RESULT AT MACH 2.5

In the useful test window of 1.66 sec the flow qualities were,

P_{0av} = 938.1 ± 7.7 [kPa] (121.41 ± 1.11 [psig]) (95%)

M_{av} = 2.48 ± 0.23%

R_{el} = 62.3(@2.63sec) ~ 63.1(@4.43sec) [10^6/m]

T_2 = -141 ~ -147 [^{o}C] (-222 ~ -233 [^{o}F])

P_2 = 57.0 ± 0.61[kPa] (8.269 ± 0.089 [psia]) (95%).

Although, the variation of the stagnation pressure is under 1 percent of the set pressure, it shows more than 1 percent of bias from the set pressure. The reason is that the pressure in the storage tube was not the same in all the runs. Another problem is seen in the stagnation pressure drop at the end of the test window. The pressure drop is an obvious indication of slow valve opening. The Mach number stays fairly constant throughout the test. The

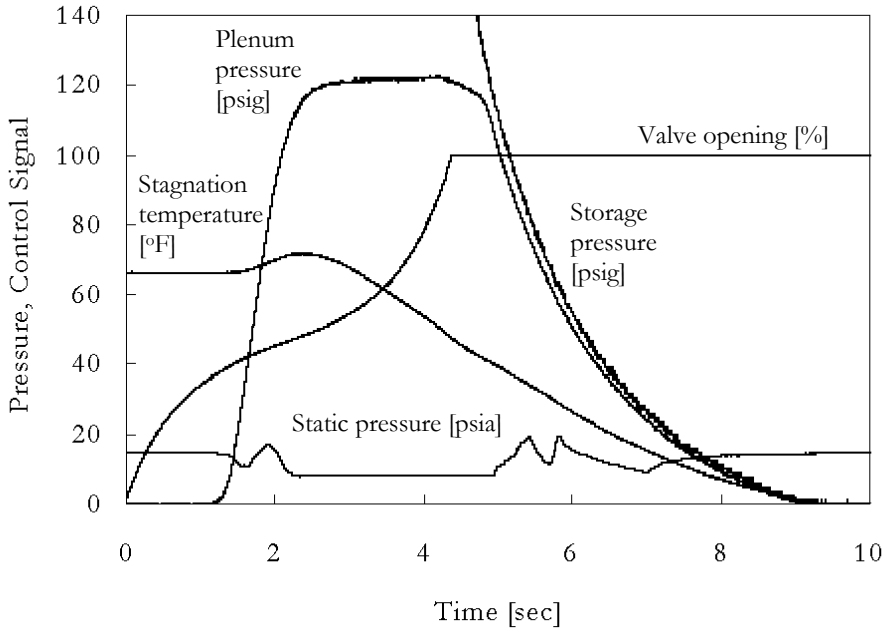

Figure 4.5. Pressure trace after training process.

stagnation temperature drops about 13 °C (25 °F) in the test window. It continuously drops until the end of the experiment. The Reynolds number increases slightly because of the stagnation temperature drop. The static pressure is rather interesting to observe. As the automatic valve starts opening, the pressure drops and rises (low speed), then it goes down to about 55 kPa (8 psia) after a normal shock passes though the nozzle. When the stagnation pressure goes down at the end of the test, the same process happens in the reverse order. This time, two oblique shocks enter the nozzle and unstart the tunnel.

The starting stagnation pressure of the tunnel was typically about 860 kPa (110 psig) for M=2.5. The pressure is much higher than the theoretical case of a normal shock is in the test section 343 kPa (35 psig), and the

minimum starting pressure of 515 kPa (60 psig) based on experiments shown in reference 3. The UT Arlington SWT requires about 80 percent more stagnation pressure to start the nozzle over a SWT with solid wall test section. There are many factors that cause the inefficiency of the tunnel. One of the primary factors is the reverse flow around the free jet, which pressurized the test section over the ambient pressure even after removing the scavenger scoop from the diffuser. This results in less pressure ratio in the supersonic nozzle. The poor design of the diffuser and the constant area duct are other factors of inefficiency. The area at exit of the diffuser and the length of the constant area duct is about quarter of typical tunnels, which also results in less pressure recovery in the diffuser.

CHAPTER 5

CONCLUSIONS AND RECOMMENDATIONS

The UT Arlington 0.15 x 0.15 m (6 x 6 in.) blowdown supersonic wind tunnel was constructed and successfully started at M=2.5 and the run time was 1.6 s. The minimum starting plenum pressure was about 860 kPa (110 psig). The High-pressure compressor provides the compressed air to the storage tube before a run. As the automatic valve is opened using the PC-based operating system, the high-pressured air expands to the plenum chamber and settles down. The turbulent flow is stabilized using three damping screens in the plenum chamber. The supersonic nozzle accelerates the air to a supersonic jet. The test section that has a larger area so that a relatively large engine models can be subjected into the jet. Downstream of the test section, the supersonic jet is decelerated by constant area diffuser and exhausted into the atmosphere.

The starting pressure was substantially higher than that of a typical wind tunnel with a solid wall test section. The excess pressure in the test section was one of the major causes. In the test section, the mixing region of surrounding air around the supersonic jet widened as the jet length increased. As the induced air encountered the converging wall of entrance section of the diffuser, it was redirected back into the test section. This problem was temporarily solved by modifying the fixed top plate of the test section to a movable pressure relief plate. To reduce the starting plenum pressure, components downstream of the test section need to be modified. The converging section after the test section must be reshaped to minimize the re-circulation of flow. The area and length of the constant area duct must be increased to reduce the static pressure in the test section.

The preprogrammed controller replaced a conventional PID controller. It was necessary because the volume of the supply air is too limited. The preprogrammed controller starts the wind tunnel in less than 1.5 s without any over or under shoot of the plenum pressure. On the contrary, it usually takes about 2 s to start and 1 s to settle down the stagnation pressure using feedback loop controller. An optimum control signal was made using six training runs and comparing the difference in pressures and output signals. The controller has a potential to keep

the fluctuation of the stagnation pressure within 1 percent of a set point pressure. To eliminate steady state deviation of the plenum pressure, the manual filling process needs to be upgraded to a computerized system. The valve opening profiles for the range of Mach numbers (M = 1.5-4.0) must be found.

To utilize the wind tunnel as experimental facility, the flow quality of the supersonic jet must be evaluated. A total pressure rake will be attached in the test section to find the axial and longitudinal Mach number distribution. Flow angularity can be measured using a pitot probe. Finally, the operating program and the program of preprogrammed controller must be integrated for ease of use.

APPENDIX A

UT ARLINGTON 6 X 6 IN. SUPERSONIC WIND TUNNEL

UT Arlington 6 x 6 in. supersonic wind tunnel

APPENDIX B

TYPE OF SIGNALS IN COMMUNICATION CABLES

Signals of 15-conductor cable

Channel	Usage
1,2	0~20mA signal from pressure transmitter (1: 24V Excitation, 2: Ground)
2,3	0~20mA signal to valve controller (1: Positive, 2: Ground)
4~15	Reserved for additional transducers

Signals of 25-conductor cable

Channel	Usage
1~3	Pressure transducer PX613-1KG5V, (1: 24VDC Excitation, 2: +out, 3: Common)
4~6	Pressure transducer PX613-300G5V, (4: 24VDC Excitation, 5: +out, 6: Common)
7~9	Pressure transducer PX613-100G5V, (7: 24VDC Excitation, 8: +out, 9: Common)
10~12	Pressure transducer PX303-050A10V, (10: 24VDC Excitation, 11: +out, 12: Common)
14~15	Thermocouple Type T (14: +out, 15: -out)
13, 16~25	Reserved for additional transducers

Input signals of PCI-MIO-16E-4

Channel	Usage
0, 8	Pressure transducer PX613-1KG5V, (0: +out, 8: GND)
1, 9	Pressure transducer PX613-300G5V, (1: +out, 9: GND)
2, 10	Pressure transducer PX613-100G5V, (2: +out, 10: GND)
3, 11	Pressure transducer PX303-050A10V, (3: +out, 11: GND)
4, 12	Thermocouple Type T
5, 13	Control signal
6, 7, 15, 16	Reserved for additional transducers

APPENDIX C

FLOWCHART OF PREPROGRAMMED CONTROLLER

Flowchart of preprogrammed controller

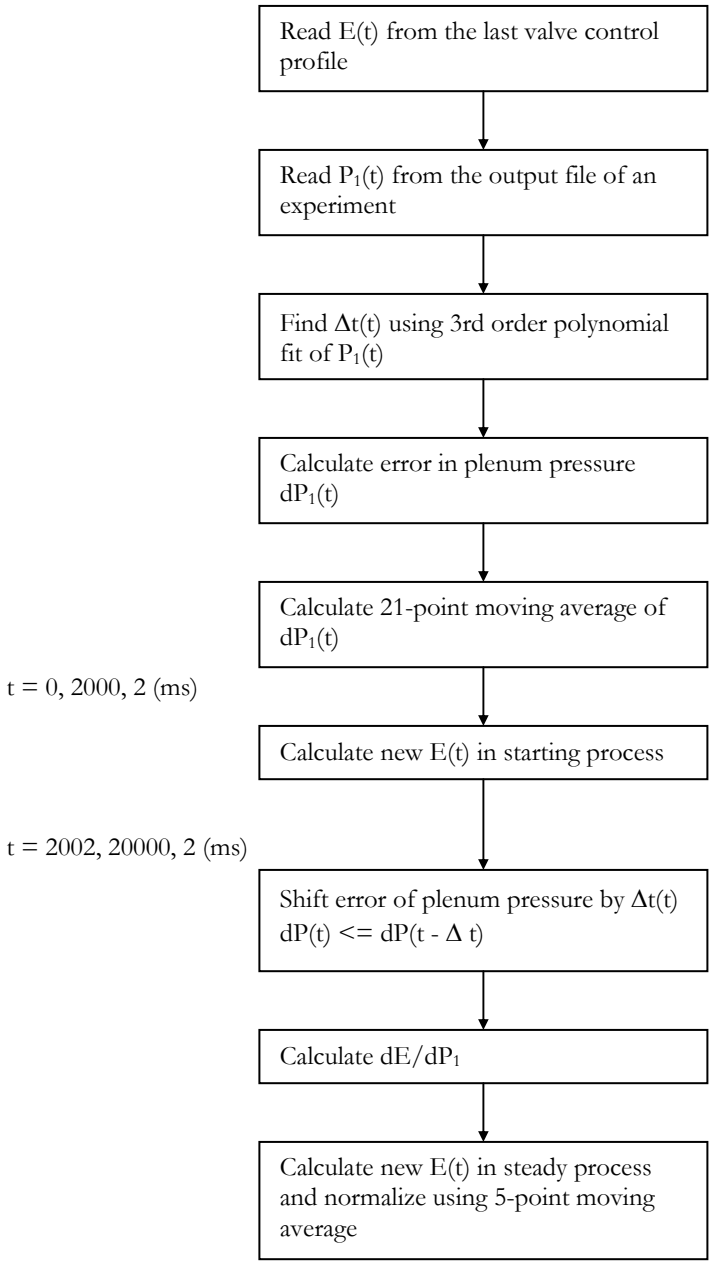

REFERENCES

[1] Anderson, J. D., *Modern Compressible Flow with Historical Perspective*, McGraw-Hill Inc., New York, 1990, pp. 1-4.

[2] Pope, A. and Goin K., *High-Speed Wind Tunnel Testing*, Wiley, New York, 1965, pp. 62-134.

[3] "Rules for Construction of Pressure Vessels – division 1," *ASME Boiler and Pressure Vessel Code*, The American Society of Mechanical Engineers, New York, 1986.

[4] Schubauer, G. B., Spangenberg, W. G., and Klebanoff, P. S., "Aerodynamic Charactoristics of Damping Screens," NACA Technical Note 2001, 1950.

[5] Lee, J. D. and Von Eschen, G. L., "Critical Performance Parameters of an Intermittent High-Pressure Free-jet Supersonic Wind Tunnel," The Ohio State University Research Foundation, July 31, 1954, pp. 20-22.

[6] Neumann, E. P. and Lustwerk, F., "Supersonic Diffusers for Wind Tunnels," *Journal of Applied Mechanics*, June 1949.

[7] Cronvich, L. L. and Faro I. D. V., "Handbook of Supersonic Aerodynamics, Section 17 Ducts, Nozzles and Diffusers," NAVWEPS Report 1488 (Vol. 6), January 1964, pp. 269-305.

[8] Liu, M., "An Open Architecture Dynamic Data Acquisition System for Wind Tunnel Testing," AIAA98-0344, 1998.

[9] Buggele, A. E. and Decker, A. J., "Control of Wind Tunnel Operations Using Neural Net Interpolation of Flow Visualization Records", NASA Technical Memorandum 106683, 1994.

[10] Arrington, E. A., Gonsalez, J.C. and Beck, E.A., "Flow Quality and Operational Enhancements in the NASA Lewis 8-by6-foot Supersonic Wind Tunnel", AIAA98-2706, 1998.

[11] Marvin, J. G., "Wind Tunnel Requirements for Computational Fluid Dynamics Code Verification", NASA Technical Memorandum 100001, 1987.

BIOGRAPHICAL STATMENT

Joji Matsumoto was born in Matsuyama, Japan in 1972. He completed Dogo elementary school in 1985, Dogo junior high school in 1988, and Matsuyama Higashi high school in 1991. He entered Kyushu University at Fukuoka, Japan in 1991 and graduated in 1995 with a Bachelor of Science in Mechanical Engineering. He started graduate studies in Aerospace Engineering at The University of Texas at Arlington in 1996 and received Master of Science in Aerospace Engineering in 2000. His area of research was in experimental aerodynamics. He is a student member of American Institute of Aeronautics and Astronautics.